3D-DCT Based Zero-Watermarking for Medical Volume Data Robust to Geometrical Attacks

Jingbing Li[1], Wencai Du[1], Yong Bai[1], and Yen-wei Chen[2]

[1] College of Information Science and Technology, Hainan University, Haikou 570228, China
[2] College of Information Science and Engineering, Ritsumeikan University, Kasatsu-shi 525-8577, Japan
Jingbingli2008@hotmail.com, wencai@hainu.edu.cn, bai@hainu.edu.cn, chen@is.ritsumei.ac.jp

Abstract. This paper presents a method for robust watermarking of medical volume data using 3D-DCT. A feature vector of the volume data is utilized to enhance the robustness against rotation, scaling, translation, and cropping changes. The proposed algorithm utilizes the volume data's feature, Hash function, the third party authentication. We describe how to obtain the feature vector of medical volume data and embed and extract the watermarking. Simulation results demonstrate the proposed algorithm's robustness against rotation up to 30°, against scaling down to 20% of the image's original size, and against translation transform up to 10%.

Keywords: 3D-DCT, Digital watermarking, Medical volume data, Robust, Geometrical attacks.

1 Introduction

With the advancing of the multimedia and internet technology, telediagnosis, telesurgery and cooperative working session have been undergoing rapid development. However, when Electronic Patient Records(EPR) and medical images are transmitted on the Internet, there may be the risk of disclosure of personal privacy[1][2]. Medical image watermarking can be a effective technology to solve this problem[3][4]. Traditionally Digital watermarking technology is used in the copyright protection of digital media first. Using watermark's properties of invisibility and robustness, patient information, doctor diagnosis and Electronic Patient Records can be used as the watermarking hidden in the CT, MRI (Magnetic Resonance Imaging) and other medical images[5].

Medical image watermarking is usually divided into three types [4].

1) RONI(Region of non-interest)-based medical image watermarking. The content of medical images can not tolerate significant changes when watermarking is embedded. Hence, the watermarking information is embedded in the RONI of the medical images[6][7]. However, the capacity of hidden information is limited because most of the RONI area of the image is the black background.

P. Sénac, M. Ott, and A. Seneviratne (Eds.): ICWCA 2011, LNICST 72, pp. 433–444, 2012.

2) Reversible watermarking. Using reversible watermarking, once the embedded content is read, the watermarking can be removed from the image allowing retrieval of the original image[8]. Unfortunately, most of the reversible watermarking is fragile. Its robustness is poor and the capacity is still way below the embedding capacity of non-reversible watermarking technique.

3) Classical watermarking. In this method, watermarking is often embedded in the least significant bit (LSB) [9], or in the low or middle frequency coefficients in the frequency domain(DCT,DFT or DWT) [10]. However, compared to the previous two methods, the capacity of the embedded watermark affects the content of Region of Interest. It is necessary to control the amount of the embedded watermarking to avoid the doctors make the wrong diagnosis. In addition, the classical watermarking has low robustness especially against geometric attacks.

2 Three Dimension Cosine Transform(3D-DCT) and Inverse Discrete Cosine Transform(3D-IDCT)

2.1 Three Dimension Cosine Transform(3D-DCT)

Three dimension cosine transform is a signal analysis theory[12][13]. The $M \times N \times P$ volume data's 3D-DCT is defined by :

$$F(u,v,w) = c(u)c(v)c(w) \cdot [\sum_{x=0}^{M-1}\sum_{y=0}^{N-1}\sum_{p=0}^{P-1} f(x,y,z) \cdot \cos\frac{(2x+1)u\pi}{2M}\cos\frac{(2y+1)v\pi}{2N}\cos\frac{(2z+1)w\pi}{2P}] \tag{1}$$

where $u = 0,1,...,M-1;\ v = 0,1,...,N-1;\ w = 0,1,...,P-1;$

$$c(u) = \begin{cases} \sqrt{1/M} & u = 0 \\ \sqrt{2/M} & u = 1,2,...,M-1 \end{cases}, \qquad c(v) = \begin{cases} \sqrt{1/N} & v = 0 \\ \sqrt{2/N} & v = 1,2,...,N-1 \end{cases}$$

$$c(w) = \begin{cases} \sqrt{1/P} & w = 0 \\ \sqrt{2/P} & w = 1,2,...,P-1 \end{cases}$$

$f(x,y,z)$ are the voxel values of volume data V at the point(x, y, z) and $F(u,v,w)$ corresponds to the 3D-DCT coefficients.

2.2 Three Dimension Inverse Cosine Transform(3D-IDCT)

The $M \times N \times P$ volume data's 3D-IDCT is defined by :

$$f(x,y,z) = \sum_{u=0}^{M-1}\sum_{v=0}^{N-1}\sum_{w=0}^{P-1}[c(u)c(v)c(w)F(u,v,w)\cos\frac{(2x+1)u\pi}{2M}\cos\frac{\pi(2y+1)v\pi}{2N}\cos\frac{\pi(2y+1)w\pi}{2N}] \tag{2}$$

where $x = 0,1,...,M-1;\ y = 0,1,...,N-1;\ z = 0,1,...,P-1$ and $c(u), c(v), c(w)$ are the same as that in the formula (1).

3 3D-DCT Based Watermarking for Medical Volume Data

3.1 A Method to Obtain the Feature Vector of Medical Volume Data

The original volume data is computed using 3D-DCT. We choose 8 low-frequency coefficients (F(1,1,1), F(1,2,1) F(2,1,1)…F(2,2,2)), shown in Table 1. We find that the value of the low-frequent coefficients may change after the image has undergone an attack, particularly geometric attacks such as rotation, scaling, and transformation. However, the signs of the coefficients remain unchanged even with strong geometric attacks, as is also shown in Table 1. The different attacked images are shown in Fig. 1(b)-(h). If "1" represents a positive coefficient, and "0" represents a negative or zero coefficient, we can then obtain the sign sequence of low-frequency coefficients, as is shown in the column "Sequence of coefficient signs" in Table 1. After attacks, the sign sequence is unchanged, and the normalized cross-correlation (NC) is equal to 1.0.

Table 1. Change of 3D-DCT low-frequency coefficients with respect to different attacks

Image Process	F(1,1,1) (10^2)	F(1,2,1) (10^2)	F(2,1,1) (10^2)	F(2,2,1) (10^2)	F(1,1,2) (10^2)	F1,2,2) (10^2)	F(2,1,2) (10^2)	F(2,2,2) (10^2)	Sequence ofcoefficient signs	NC
Original image	145.11	5.32	-36.2	-1.53	9.81	-3.33	4.23	1.52	1100 1011	1.0
Gausian noise (3%)	225.02	4.30	-26.60	-1.45	7.24	-2.03	3.04	1.03	1100 1011	1.0
JPEG (4%);	154.70	4.76	-32.54	-1.50	10.04	-3.13	4.88	1.76	1100 1011	1.0
Median filter [3x3]	146.06	5.35	-36.47	-1.61	9.67	-3.42	4.62	1.54	1100 1011	1.0
Rotation (20°)	145.10	18.13	-32.66	-16.94	9.81	-4.21	2.81	0.01	1100 1011	1.0
Scaling (x0.5)	72.67	2.67	-18.12	-0.76	4.93	-1.67	2.12	0.76	1100 1011	1.0
Translation (8%)	141.71	5.21	-69.74	-2.76	8.97	-3.32	3.04	2.39	1100 1011	1.0
Cropping (10%,from z)	142.54	4.72	-34.22	-1.24	0.73	-3.34	5.07	1.40	1100 1011	1.0

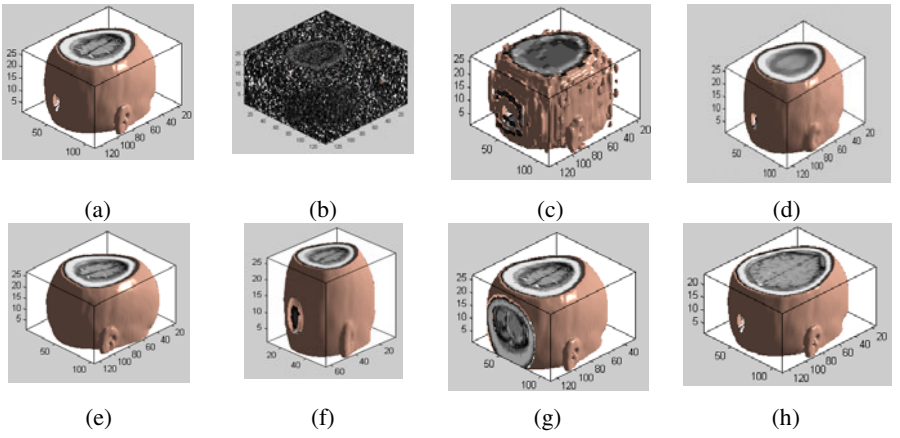

Fig. 1. Common and geometrical attacks to volume data: (a) Original volume data; (b) Gaussian noise(3%); (c) JPEG compression(4%); (d) Median filter[3x3]; (e) Rotation(20 ° clockwise); (f) Scaling(0.5times); (g) Translation(8%,down); (h) Cropping(10%,from z direction).

To prove that these sequences of coefficient signs can serve as the feature vector of medical volume data, we choose several common volume data, as shown in Fig. 2(a)-(e). After 3D-DCT, we choose 64 low-frequency coefficients--(F(1,1,1), F(1,2,1) F(2,1,1)…F(4,4,4). The 64-bit sequence of signs is then obtained and the NC is calculated. The values of NC between sequence of signs are shown in Table 2. We find that the NC values are very small (less than 0.28). This means that the sequence of signs can be regarded as the feature vector of the volume data.

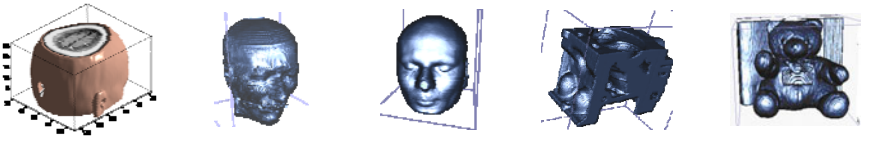

Fig. 2. 3D images of different volume data ; (a) volume data_1; (b) volume data_2; (c) volume data_3; (d) volume data_4; (e) volume data_5

Table 2. The NC values between 64-bit feature vectors of volume data

	V1.V2	V1.V3	V1.V4	V1.V5	V2.V3	V2.V4	V2.V5	V3.V4	V3.V5	V4.V5
NC	-0.31	-0.21	0.21	-0.15	0.28	-0.15	-0.09	-0.25	-0.12	0.06

3.2 Watermarking Algorithm That Uses Feature Vectors

A group of independent binary pseudomorph sequences is generated for the watermarking. The group of sequences is described as: $W=\{w_{(j)} | w_{(j)}=0,1; \quad 1 \le j \le L\}$. A volume data of size of 128×128x27 is selected as the original volume data. It is

described as: $F=\{f_{(i,j,k)} \mid f_{(i,j,k)} \in R;\quad 1 \le i \le M 1 \le j \le N, 1 \le k \le P\}$, where $f_{(i,j,k)}$ denotes the voxel values of volume data V at the point (i,j,k).

1）Embed the watermarking into the volume data

Step 1: Acquire the feature vector of the volume data using 3D-DCT

DCT of the whole F(i,j,k) is computed, and the 3D-DCT coefficient matrix, FD (i,j,k), is acquired. Then, the frequency sequence *Y(j)* –from low to high frequency– can be obtained. Finally, The feature vector $V=\{v(j) \mid v(j)=0,1; 1 \le j \le J\}$, consists of the sequence of signs of the low-frequency 3D-DCT coefficients, where the value of J can tune the robustness and capability of the embedded watermarking (in this paper we set J = 125=5x5x5 bits). Procedure is described as:

$$FD(i,j,k) = DCT3(F(i,j,k)); \tag{3}$$

$$V(j) = Sign(FD(i,j,k)); \tag{4}$$

Step 2 : Utilizing the watermarking W and volume data V, we can generate the logical sequence, *Key(j)*

$$Key(j) = V(j) \oplus W(j); \tag{5}$$

where *V(j)* denotes the feature vector of volume data, *W(j)* denotes the watermarking to be embedded, and "⊕" is the exclusive-OR operator. The binary logical sequence, *Key (j)*, can be computed. The *Key(j)* should be stored, as it is necessary to extract the watermarking. Furthermore, *Key(j)* can be regarded as a secret key and registered to the third part to preserve the ownership of the original image [14].

2) Extract the watermarking from the tested Volume data

Step 3: Using the 3D-DCT of the whole tested Volume data F'(i,j,k) and acquire the feature vector V'(j)

This process of acquiring the feature vector V' is similar to step 1 of the above algorithm for embedding the watermarking. The obtained feature vector is $V'=\{v'(j) \mid v'(j)=0,1; 1 \le j \le J\}$, which consists of the sequence of signs of the 3D-DCT coefficients and where J has the same meaning as previously.

Procedure is described as follows：

$$FD'(i,j,k) = DCT3(F'(i,j,k)); \tag{6}$$

$$V'(j) = Sign(FD'(i,j,k)); \tag{7}$$

Step 4: Extracting W'(j)

$$W'(j) = V'(j) \oplus Key(j); \tag{8}$$

where W'(j) is the extracted watermarking, V' (j) is the feature vector of the tested volume data, and Key(j) was obtained from the above process of embedding watermarking. The NC between W and W' is then computed. Finally, we can extract the hidden information from the volume data.

Furthermore, the hidden information(watermarking) can be extracted without the original data, which is advantageous to protect the safety of the medical volume data.

4 Experiments

In our experiments, 1000 groups of independent binary pseudomorph sequences are used. Every sequence consists of 125 bits. One group is selected at random from the 1000 groups as the embedded watermarking (in this paper, the 500th group is selected). Fig. 4(a) shows the original medical volume data of size 128×128x27. In order to measure the quantitative similarity, the normalized cross-correlation (*NC*) is used in this paper, defined as:

$$NC = \sum_i \sum_j [W(i,j) \cdot W'(i,j)] \Big/ \sum_i \sum_j [W(i,j)]^2 \tag{9}$$

where W denotes the embedded watermarking and W' denotes extracted watermarking.

The higher the *NC* value, the more similarity there is between the embedded and extracted watermarking. In this paper, we use the peak signal to noise ratio (PSNR) to measure the distortion of the watermarked image, defined as:

$$PSNR = 10 \log_{10} \left[\frac{\sum v_{\max}^2}{\sum (v_i' - v_i)^2} \right] \tag{10}$$

where v_i and v_i' denote the ith-voxel(or ith-pixel) values of the original volume V and watermarked V' ,respectively.

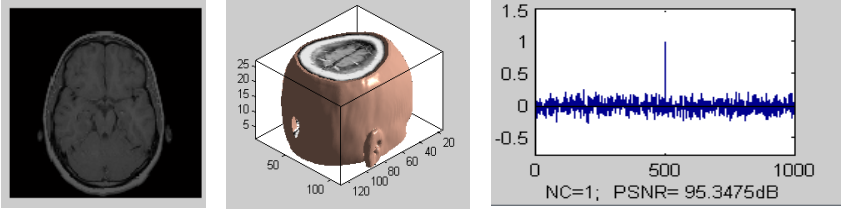

(a) (b) (c)

Fig. 3. The watermarked medicine volume data without attacks: (a) a slice of medicine volume data; (b)The corresponding 3D medical image ; (c) watermarking detector.

Fig. 3(a) shows a slice of medicine volume data without attacks. In this paper, the default is to select the tenth slice. Fig. 3(b) shows the watermarked medicine volume data (Three-dimensional) without attacks. Fig. 3(c) gives the response of the watermarking detector. The only group of binary pseudomorph sequences that responds is the one that is watermarked. The value of NC is up to 1.0, so the watermarking is obviously detected.

4.1 Common Attacks

(1) Adding Gaussian noise

The slice data under Gaussian attacks (20%) is shown in Fig. 4(a); The corresponding volume data with PSNR of 0.79 dB and NC of 0.61 is shown in Fig. 4(b). The watermarking can be detected, as shown in Fig. 4(c). Table 3 gives the PSNR and NC when the volume data have been added noise by different parameters. The result shows that the NC is 0.58 when the noise parameter is up to 25%. The watermarking can still be detected.

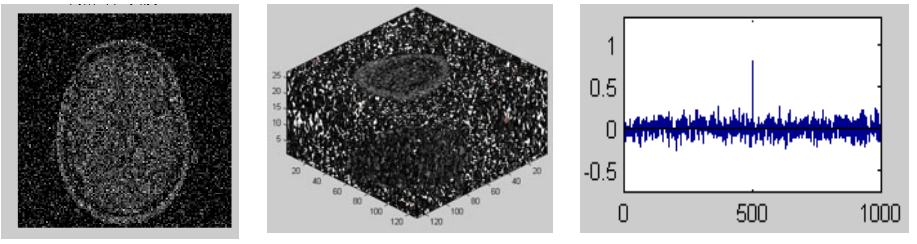

(a) (b) (c)

Fig. 4. Under noise attack(20%): (a) a slice under noise attack; (b) the corresponding 3D medical image; (c) watermarking detector

Table 3. The PSNR and NC under noise attack

Noise parameters (%)	1	3	5	10	15	20	25
PSNR(dB)	12.50	8.02	6.01	3.31	1.79	0.79	0.09
NC	0.86	0.81	0.79	0.77	0.71	0.61	0.58

(2) Filter Processing

The slice data under median filter attacks[5x5] is shown in Fig. 5(a); The corresponding volume data with PSNR of 18.68 dB and NC of 0.90 is shown in Fig. 5(b). The watermarking can be detected, as shown in Fig. 5(c). Table 4 gives the PSNR and NC under different median filter parameters. The results show that the watermarking algorithm is robust to median filter.

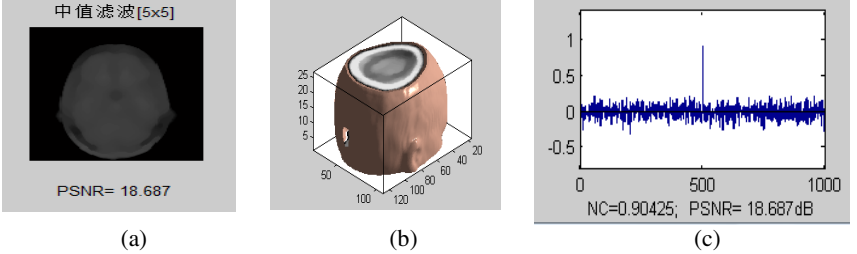

(a) (b) (c)

Fig. 5. Under filter attacks[5x5]: (a) a slice with filter attack; (b) the corresponding 3D medical image; (c) watermarking detector

Table 4. The PSNR and NC under median filtering

	Media filter[3x3]			Media filter [5x5]			Media filter [7x7]		
Repeat times	1	10	20	1	10	20	1	2	10
PSNR(dB)	24.64	22.45	21.97	21.14	18.67	18.07	18.91	18.32	16.97
NC	0.93	0.93	0.93	0.89	0.90	0.88	0.92	0.93	0.87

(3) JPEG attacks

The slice data under JPEG attacks (4%) is shown in Fig. 6(a). The corresponding volume data with PSNR of 17.82 dB and NC of 0.83 is shown in Fig. 6(b). The watermarking can be detected, as shown in Fig. 6(c). Table 5 gives the PSNR and NC under different compression quality. The result shows that the NC is 0.84 when the compression quality is down to 2%. The watermarking can still be detected. The results show that the watermarking algorithm is robust to JPEG attacks.

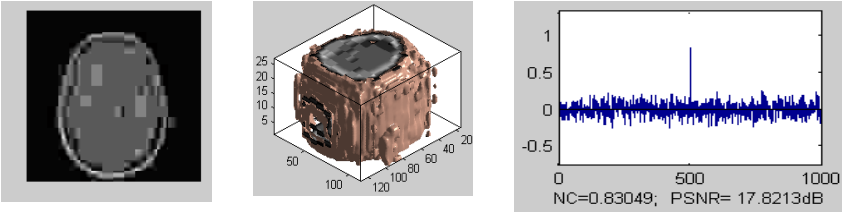

(a) (b) (c)

Fig. 6. Under JPEG attacks(4%): (a) a slice under JPEG attacks; (b) the corresponding 3D medical image; (c) watermarking detector

Table 5. The PSNR and NC under JPEG attacks

Compression Quality(%)	2	4	8	10	20	40	60	80
PSNR(dB)	16.57	17.82	20.21	21.19	23.10	25.06	26.61	29.30
NC	0.84	0.83	0.90	0.91	0.91	0.96	0.96	0.93

4.2 Geometrical Attacks

(1) Rotation attacks

Fig. 7(a) and Fig. 7(b) show the slice and volume data rotated clockwise by 20°, respectively. PSNR and NC are 12.44dB and 0.66, respectively. The watermarking can be detected, as shown in Fig. 7(c). Table 6 gives the PSNR and NC when the volume data has been rotated by different angles. The results show that the NC is 0.53 when the angle of rotation is up to 30°. The watermarking can still be detected. In [15] a watermarking was embedded in DFT domain, however, the maximum angle of rotation is not greater than 3°. Therefore we can conclude that our scheme is robust against rotation attacks.

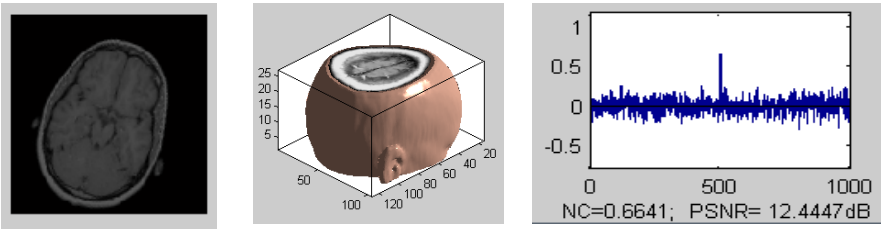

(a) (b) (c)

Fig. 7. Rotation attack (angle is 20°): (a) a slice with rotation attack; (b) the corresponding 3D medical image; (c) watermarking detector.

Table 6. The PSNR and NC under rotation attacks

Rotation	0º	5º	10º	15º	20º	25º	30º	35º
PSNR(dB)		16.53	13.96	12.97	12.44	12.04	11.67	11.33
NC	1.00	0.79	0.76	0.69	0.66	0.56	0.53	0.45

(2) Scaling attacks

Fig. 8(a) and Fig. 8(b) show the slice and the corresponding 3D medical image shrunk with a scale factor of 0.5, respectively.

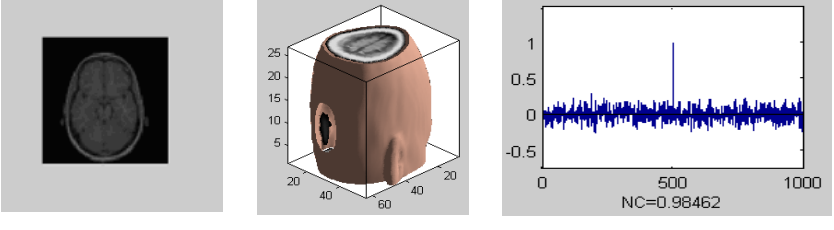

(a) (b) (c)

Fig. 8. Scaling attack (scaling factor 50%): (a) a slice with scaling attack; (b) the corresponding 3D medical image; (c) watermarking detector

Fig. 8(c) shows that the watermarking with a NC of 0.84 can be detected. Table 7 contains the NC value when the image has been scaled. If the scale factor drops to 0.2, then the NC value is 0.82. Therefore, our algorithm is robust to scaling attacks.

Table 7. The NC under scaling

Scaling factor	0.2	0.5	0.8	1.0	1.2	2.0	4.0
NC	0.82	0.98	0.90	1.0	0.96	0.98	0.98

(3) Translation attacks

Fig. 9(a) and Fig. 9(b) show the slice and the corresponding 3D medical image translated by 10 % vertical translation down, respectively. The PSNR and NC are 10.84dB and 0.56, respectively. Fig. 9(c) shows that the watermarking can be

detected. Table 8 contains the values of PSNR and NC when the image has been translated. The results show that the scheme is robust against translation.

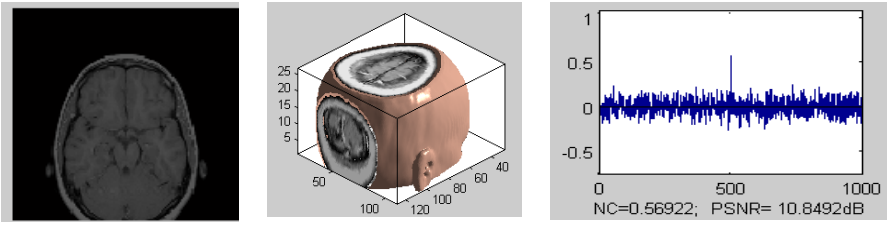

(a) (b) (c)

Fig. 9. Translation transforms (translation 10%): (a) a slice with translation attack; (b) the corresponding 3D medical image; (c) watermarking detector.

Table 8. The PSNR and NC under translation

	Horizontal translation(Left)			Vertical translation(Down)		
Distance (pixels)	6	8	10	6	8	10
PSNR (dB)	11.13	10.43	9.99	11.65	11.09	10.84
NC	0.61	0.58	0.55	0.82	0.68	0.56

(4) Cropping attacks

Fig. 10(a) and Fig. 10(b) show the slice and the corresponding medical volume data cropping from z axis at the ratio of 10 %, respectively. The NC is 0.77. Fig. 10(c) shows that the watermarking can be detected. Table 9 contains the values of NC when the image has been cropped. The results show that if the watermarked volume data is cropped by 14 % from z axis, then we can obtain NC of 0.71. Therefore, the watermarking is still detected. The results show that the proposed algorithm is robust against cropping attacks.

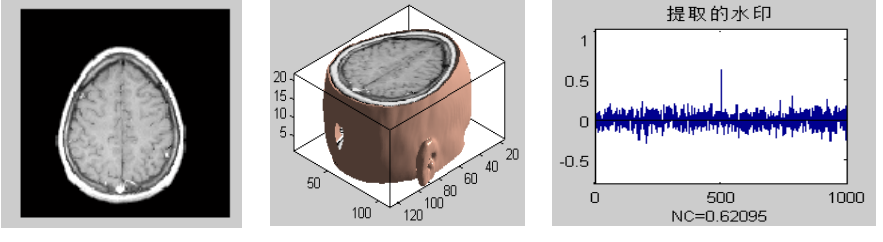

(a) (b) (c)

Fig. 10. Cropping (From the Z axis,10%): (a) the first slice after cropping; (b) the corresponding 3D medical image; (c) watermarking detector

Table 9. The NC under cropping

Cropping ratio	2%	4%	6%	8%	10%	12%	14%
NC(cropping from Z)	0.91	0.91	0.84	0.84	0.77	0.77	0.71
NC(cropping from Y)	0.95	0.90	0.82	0.79	0.71	0.68	0.63
NC(cropping from X)	0.86	0.72	0.66	0.64	0.61	0.55	0.52

(5) Distortion attacks

Fig. 11(a) and Fig. 11(b) show the slice and the corresponding 3D medical image under distortion attacks with the factor of 13, respectively. The PSNR and NC are 9.83dB and 0.60, respectively. Fig. 11(c) shows that the watermarking can be detected. Table 10 contains the values of PSNR and NC when the image has been distorted. The results show that the scheme is robust against distortion.

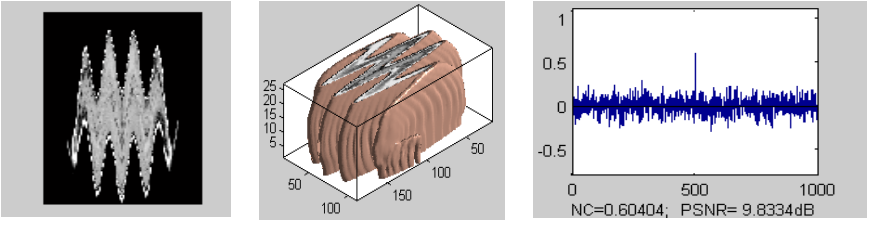

(a) (b) (c)

Fig. 11. Distortion attacks (factor is 13): (a) a slice under distortion attacks; (b) the corresponding 3D medical image; (c) watermarking detector

Table 10. The PSNR and NC under distortion attacks

Distortion factor	5	7	9	11	13	15	17	20	22	24	26
PSNR(dB)	10.16	9.88	9.58	9.43	9.83	9.7	9.8	9.68	9.77	9.68	9.68
NC	0.42	0.40	0.52	0.44	0.60	0.55	0.56	0.58	0.58	0.66	0.63

5 Conclusion

A novel embedding and extracting algorithm is presented in this paper. The algorithm is based on 3D-DCT. It combines feature vector, Hash function, the third party authentication. The watermarking can be extracted without the original medical volume data. Experimental results show that the algorithm is robust to geometric attacks including rotation, scaling and translation and cropping. Moreover, the content of medical volume data remains unchanged with our proposed algorithm which is one kind of the zero-watermarking technology.

Acknowledgements. This work is partly supported by Hainan University Graduate Education Reform Project (yjg0117), and by Natural Science Foundation of Hainan Province (60894), and by Education Department of Hainan Province project (Hjkj2009-03), and by Communication and Information System, Hainan University -- Institute of Acoustics, Chinese Academy of Sciences for Joint Training of Special Support.

References

1. Coatrieux, G., Lecornu, L.: A Review of Image Watermarking Applications in Healthcare. In: Proc. 28th Annual International Conference of the IEEE: Engineering in Medicine and Biology Society, EMBS 2006, pp. 4691–4694 (2006)
2. Woo, C.-S., Du, J., Pham, B.: Multiple Watermark Method for Privacy Control and Tamper Detection in Medical Images. In: Proc. APRS Workshop on Digital Image Computing Pattern Recognition and Imaging for Medical Applications, pp. 43–48 (2005)
3. Navas, K.A., Sasikumar, M.: Survey of Medical Image Watermarking Algorithms. In: 4th International Conference: Sciences of Electronic, Technologies of Information and Telecommunications, TUNISIA, March 25-29 (2007)
4. Coatrieux, G., Maître, H., Sankur, B., Rolland, Y., Collorec, R.: Relevance of watermarking in medical Imaging. In: Proc. IEEE Int.Conf. ITAB, USA, pp. 250–255 (2000)
5. Rajendra Acharya, U., Niranjan, U.C., Iyengar, S.S., Kannathal, N., Min, L.C.: Simultaneous storage of patient information with medical images in the frequency domain. Computer Methods and Programs in Biomedicine 76, 13–19 (2004)
6. Coatrieux, G., Sankur, B., Maître, H.: Strict Integrity Control of Biomedical Images. In: Proc. Electronic Imaging, Security and Watermarking of Multimedia Contents, SPIE, USA, pp. 229–240 (2001)
7. Wakatani, A.: Digital watermarking for ROI medical images by using compressed signature image. In: Proc. 35th Hawaii International Conference on System Sciences, pp. 2043–2048 (2002)
8. Macq, B., Dewey, F.: Trusted Headers for Medical Images. In: DFG VIII-DII Watermarking Workshop, Erlangen, Germany (1999)
9. Zhou, X.Q., Huang, H.K., Lou, S.L.: Authenticity and integrity of digital mammography images. IEEE Trans. on Medical Imaging 20(8), 784–791 (2001)
10. Cox, I.J., Miller, M.L.: The first 50 years of electronic watermarking. Journal of Applied Signal Processing (2), 126–132 (2002)
11. Wu, Y.H., Guan, X., Kankanhalli, M.S., Huang, Z.Y.: Robust Invisible Watermarking of Volume Data Using 3D DCT[A]. In: Proceedings of Computer Graphics International, vol. 3(6), pp. 359–362. IEEE Computer Society Press, Hong Kong (2002)
12. Liu, W., Zhao, C.: Digital watermarking for volume data based on 3D-DWT and 3D-DCT. In: Proceedings of Int. Conf. Interaction Sciences, pp. 352–357 (2009)
13. Rao, K., Yip, R.: Discrete cosine transform: algorithms, advantages, applications. Academic Press Inc., London (1990)
14. Jeng-Shyang, P., Hsiang-cheh, H., Feng, W.: A VQ-based multi-watermarking algorithm. In: Proceedings of IEEE TENCON, pp. 117–120 (2002)
15. Solachidis, V., Pitas, I.: Circularly symmetric watermark embedding in 2-D DFT domain. IEEE Tranactions on image processing 10(11), 1741–1753 (2001)